Semiconductor Physics, Quantum Electronics & Optoelectronics, 2023. V. 26, No 1. P. 114-119.

Optoelectronics and optoelectronic devices

Utilizing machine learning algorithm in predicting the power conversion efficiency limit of a monolithically perovskites/silicon tandem structure

M. Ganoub[1], O. Al-Saban[2], S.O. Abdellatif [2*], K. Kirah[3], H.A. Ghali[2]

[1]*The Renewable Energy Postgraduate programme and the FabLab in the Centre for Emerging Learning Technologies (CELT), The British University in Egypt (BUE), El-Sherouk 11837, Cairo, Egypt*
[2]*FabLab in the Centre for Emerging Learning Technologies (CELT), Electrical Engineering Department, Faculty of Engineering, The British University in Egypt (BUE), El-Sherouk 11837, Cairo, Egypt*
[3]*Engineering Physics Department, Faculty of Engineering, Ain Shams University, Cairo, Egypt*
[*]*Corresponding author e-mail: Sameh.osama@bue.edu.eg*

Abstract. Tandem structures have been introduced to the photovoltaics (PV) market to boost power conversion efficiency (PCE). Single-junction cells' PCE, either in a homojunction or heterojunction format, are clipped to a theoretical limit associated with the absorbing material bandgap. Scaling up the single-junction cells to a multi-junction tandem structure penetrates such limits. One of the promising tandem structures is the perovskite over silicon topology. Si junction is utilized as a counter bare cell with perovskites layer above, under applying the bandgap engineering aspects. Herein, we adopt $BaTiO_3$/$CsPbCl_3$/$MAPbBr_3$/$CH_3NH_3PbI_3$/c-Si tandem structure to be investigated. In tandem PVs, various input parameters can be tuned to maximize PCE, leading to a massive increase in the input combinations. Such a vast dataset directly reflects the computational requirements needed to simulate the wide range of combinations and the computational time. In this study, we seed our random-forest machine learning model with the 3×10^6 points' dataset with our optoelectronic numerical model in SCAPS. The machine learning could estimate the maximum PCE limit of the proposed tandem structure at around 37.8%, which is more than double the bare Si-cell reported by 18%.

Keywords: tandem solar cells, numerical modeling, perovskites, random-forest algorithm, crystalline silicon.

https://doi.org/10.15407/spqeo26.01.114
PACS 88.40.H-

Manuscript 16.01.23; revised version received 28.02.23; accepted for publication 08.03.23; published online 24.03.23.

1. Introduction

Boosting solar cell power conversion efficiency (PCE) is a global challenge in the research community [1–4]. Such boosting can be implemented on a mono-junction cell level [5, 6] regarding new materials and/or structures. Alternatively, enhancing PCE by integrating multi-junctions in the form of tandem cells [1, 7–10]. Basically, tandem structures record is relatively higher than that of PCE concerning mono-junctions, which can exceed the theoretical limit associated with mono-junction cells [11, 12]. Various multi-junction tandem structures have been reported in the literature, seeking maximum PCE, robust stability, and minimum cost [11]. Among various topologies, combining perovskites with Si, it has been reported a considerable potential for high-efficiency tandem cells [1, 9–14]. On the one hand, utilizing silicon as a counter cell increases the robustness of the tandem structure as a stable cell. On the other hand, perovskites' front layer(s) can maximize the captured photons by bottom-up bandgap widening.

Although tandem structures demonstrate ultra-high capabilities to maximize PCE of tandem cells, the optimization process for such structures is a real challenge [1, 10, 11]. This is due to the nature of this structure containing a series of cascaded layers, where each layer has its internal optimization parameters, *i.e.*, thickness, doping, defects, *etc*. Additionally, the coupling parameters between layers boundaries contribute to the overall PCE calculations. Accordingly, the parameters associated with PCE maximization are substantial, making it inapplicable to tackle the optimization experimentally. Based on that, numerical techniques are commonly used to investigate large input combinations [1, 9–11, 14]. Most probably,

this numerical optimization process requires high computational resources and considerable computing time. In addition, these numerical optimizers consider minimal inputs, for example, the front electrode [10] or a single layer in the cascaded structure [14].

With the aid of a machine and deep learning, the solar cells in general, and tandem cells in particular, can be optimized [7, 15]. In addition, some reported literature has shown the utilization of machine and deep learning algorithms to predict cell efficiencies. Integration of the machine learning (ML) algorithm facilitates optimization of the process, especially for sophisticated tandem structures, as well as enables the prediction capabilities, beyond the range of the input dataset.

In this study, we provide an attempt to optimize a counter Si cell used for perovskite/Si tandem structure to maximize the output power conversion efficiency. The study highlights the ranking of several inputs in terms of their contribution to PCE as the main output. Single and multi-dimension optimization curves are plotted, seeking an optimum Si-based cell. Consequently, the overall perovskite/Si cell has been simulated with all the corresponding macroscopic parameters.

2. Optoelectronic, machine learning models, and dataset generation

The optoelectronic and carrier transport modeling for the perovskite/Si tandem cell is performed using SCAPS [16–20]. SCAPS model solar cells as a cascaded layer, with each of a given optoelectronic properties, see schematic in Fig. 1, and data in Table. The front perovskite structure is chosen to be: $BaTiO_3$/$CsPbCl_3$/$MAPbBr_3$/$CH_3NH_3PbI_3$. The front perovskite structure is cascaded from the counter side by a crystalline silicon cell with an n^{++}-n-p^{++} junction. The AM1.5G spectrum optically injects the overall tandem structure under the one Sun condition.

Recently, ML algorithm has been effectively integrated into various semiconductor and optoelectronics materials and device optimization and prediction [21–24]. This is usually tagged under the name of material informatics or devices informatics. As mentioned earlier, this paper focuses on optimizing the structure in terms of the counter bare Si silicon. We investigate PCE of the Si cell due to variations of both doping and thickness for the n-region and highly doped n^{++}-region.

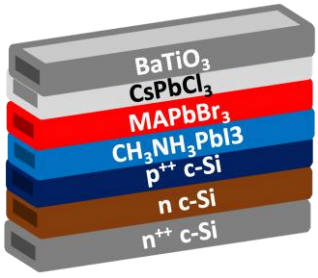

Fig. 1. The schematic for perovskite/Si tandem cell consists of $BaTiO_3$/$CsPbCl_3$/$MAPbBr_3$/$CH_3NH_3PbI_3$/c-Si tandem cell.

Table. Input material parameters for the c-Si bare cell. The cell was selected to represent the experimental work reported in [27].

Material/Parameter	n^{++}-c-Si	n-c-Si	p^{++}-c-Si
Thickness (μm)	0.05	220	0.1
Concentration (cm^{-3})	donors $8.75\cdot10^{17}$	donors $2.00\cdot10^{14}$	acceptors $1.70\cdot10^{16}$

Herein, we promote these four inputs from a series of simulations using SCAPS to capture the main contributing design parameters to PCE. The dataset combing four inputs along with PCE as output is listed to be seeded in a random-forest machine learning model.

In this study, we apply a random forest ML algorithm to optimize the Si counter cell. Random forest (RF) is a supervised machine learning algorithm, and its primary usage is in machine learning problems of classification and regression [25]. Random forest is a decision-tree-based algorithm; it operates using multiple decision trees that run in parallel with each other, preventing any interaction between them from ensuring that the analysis of each decision tree is not affected by the other trees. This method of combining the analysis of multiple algorithms to generate a more accurate result is called “Ensemble Learning”. Another critical aspect of the Random forest algorithm is its randomization capabilities, also named Bootstrap Aggregation or Bagging [25]. The Bagging method allows the random sampling of data points before using the decision-tree algorithm. Moreover, bagging is random sampling with replacement, which means that bagging could sample some of the data points more than once; which decreases the bias in the sampled data points, prevents over-fitting, as well as reduces the variance of the algorithm [25]. Thus, it solves the disadvantage of using multiple decision trees, as the decision-tree algorithm usually has a high variance value due to its sensitivity to small changes in the input values [25, 26].

3. Simulation results and discussion

This section demonstrates all the results extracted from the ML algorithm, seeded by the dataset implemented using SCAPS. The random forest model’s training capabilities should be tested and validated as represented in Fig. 2. The model recorded 99.3% overall prediction accuracy, with a maximum root mean square error deviation of 0.367%. As stated earlier, in tandem structure, significantly, with multi-cascaded junctions, the input parameters that can contribute to PCE increase considerably. However, the contribution of these inputs to PCE is not equally weighted. Primitively, we use SCAPS to narrow down the dominating input contribution list. It was observed that the bare silicon cell parameters, especially the n-doped regions, dominate the overall tandem cell PCE. Accordingly, the thickness and doping of the n^{++}- and n-regions are selected as the primary input parameters against the overall PCE.

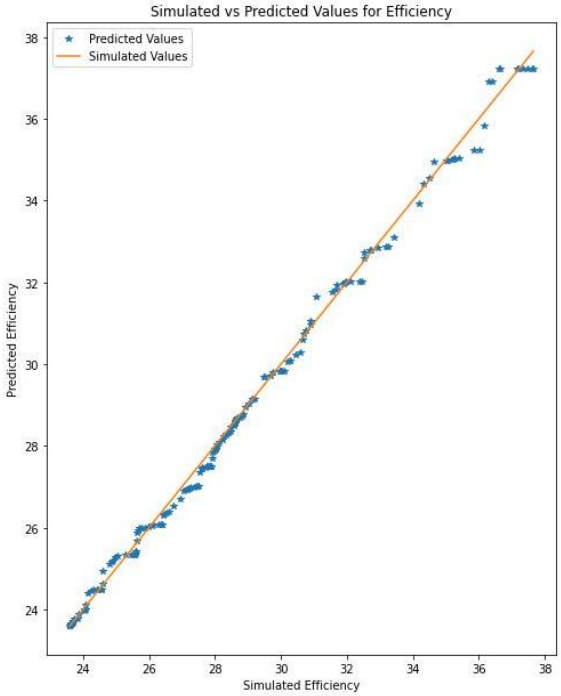

Fig. 2. The overall fitting accuracy for the proposed random-forest model by using the dataset extracted from SCAPS for the tandem structure.

Obviously, by observing Fig. 3, a direct proportionality between each of the four inputs and PCE is recorded. This reflects the basic semiconductor understanding concerning the impact of increasing either the doping or thickness in enhancing the dominating carrier, electrons, in this case, densities. This increasing trend is followed by saturation, as in Fig. 3d, or sometimes degradation. The saturation, or even reduction, is a function of the reduction in mobility due to the higher density of impurities as well as the domination of the recommendation effect. Regardless of the expected standard behavior shown in Fig. 3, the main point is that these inputs contribute equality to PCE? Answering this question impacts the capabilities to boost the overall PCE of the tandem structure.

One of the main advantages of the random forest machine learning model is that it not only allows predicting the tandem cell performance under a wide range of input conditions but also ranks the input in terms of its contribution to PCE as the main output. The chart in Fig. 4 highlights the importance level for the selected four inputs on PCE of the cell. Here, it can be observed that the doping of the *n*-region is the main dominating parameter in PCE. We can attribute this to the cortical role of the *n*-region sandwiched between the two high-doped regions. The *n*-region is considered as the main

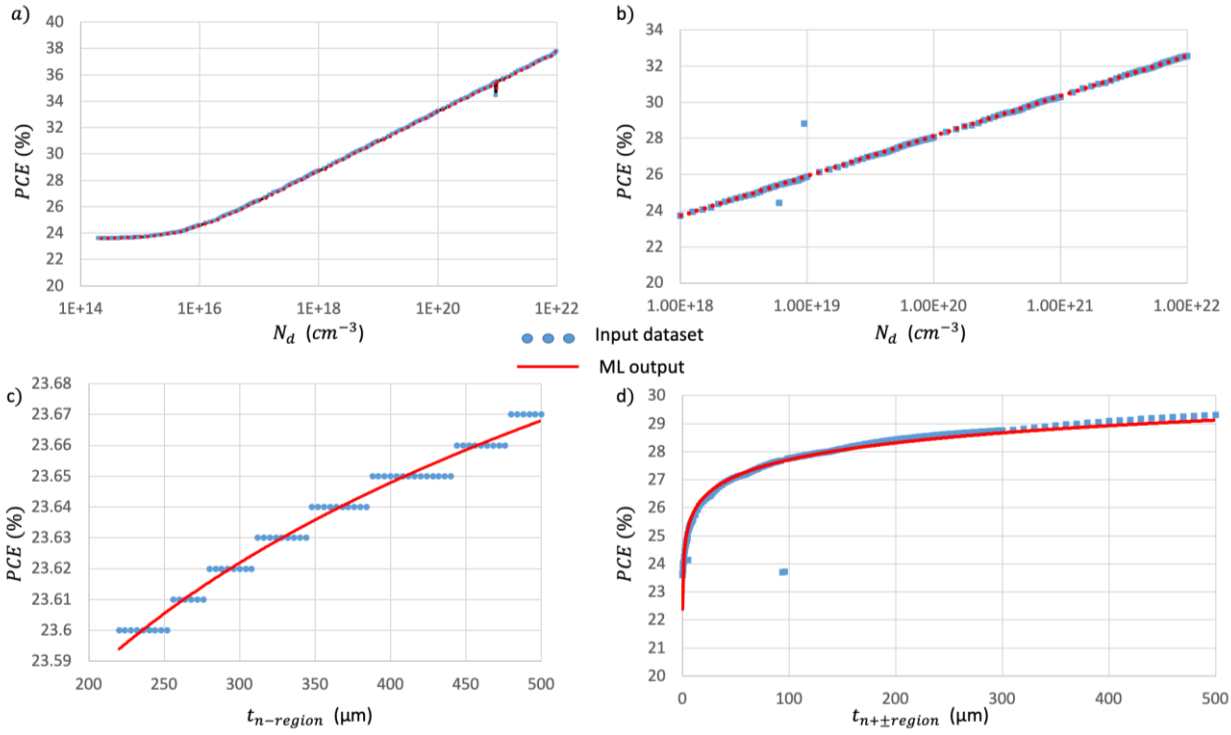

Fig. 3. Variation of four selected inputs against PCE of the tandem cell, with the ML fitting model: (a) *n*-region doping under n^{++}-doping of $8.75 \cdot 10^{21}$ cm^{-3}, with 0.1-µm thickness, while the *n*-region is of 220-µm thickness, (b) n^{++}-doping impact on PCE, under *n*-region doping of $2 \cdot 10^{14}$ cm^{-3}, with 220-µm thickness, while the n^{++}-region of 0.1-µm thickness, (c) *n*-region thickness influence on PCE under n^{++}-doping of $8.75 \cdot 10^{21}$ cm^{-3}, with 0.1-µm thickness, while the *n*-region doping reaches $2 \cdot 10^{14}$ cm^{-3}, and (d) n^{++}-thickness impact on PCE, under *n*-region doping of $2 \cdot 10^{14}$ cm^{-3}, with 220-µm thickness, while the n^{++}-region doping reach $8.75 \cdot 10^{21}$ cm^{-3}.

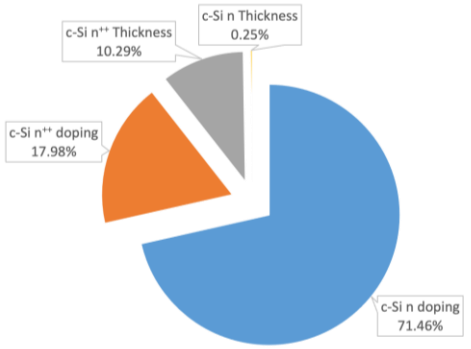

Fig. 4. Contribution level of the four selected inputs on PCE of the tandem cell.

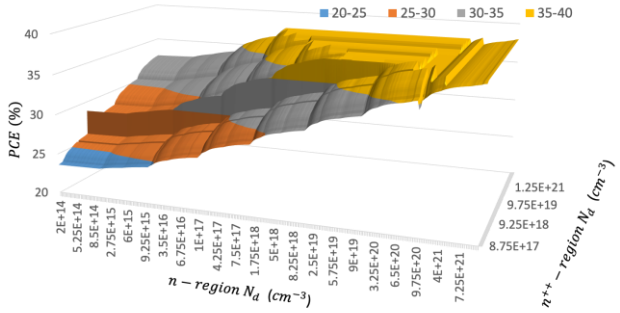

Fig. 5. Impact of the doping in both *n*- and n^{++}-regions on PCE of tandem cells. The ML prediction curve is under the *n*-region thickness close to 500 μm, for the n^{++}-region thickness of 300 μm.

absorbing layer in the c-Si bare cell. In other words, this layer compensates for the role of the intrinsic layer in the standard *p*-*i*-*n* junction cell – the *n*-region layer already with relatively high thickness, a minimum of 200 μm. Accordingly, the effect of thickness is relatively diluted, as it is already beyond the absorption length of Si. This promotes doping to be the main contributing parameter.

In addition to the *n*-region doping, the n^{++}-region doping and thickness were recorded. For the second and third places of importance, see Fig. 4. The n^{++}-region acts as the stock for electrons in the n^{++}-*n*-p^{++} junction. Knowing that the sandwiched layer is *n*-doped led to an asymmetric junction, biased towards electrons rather than holes. In other words, a bipolar junction, with dominating electrons, contributes to current density rather than holes. Again, the doping contribution in the n^{++}-region has a slightly higher effect than the same layer thickness. However, the n^{++}-region thickness is significantly cortical, while referencing the *n*-region thickness.

The importance level shown in Fig. 4 indicated the critical role of doping in both *n*- and n^{++}-regions on PCE of the tandem cell. Consequently, the variation of both doping is investigated in PCE in the 3D plot in Fig. 5. The increasing trend shown in the beginning reflects the same behavior demonstrated in Fig. 3. Interestingly, PCE recorded a saturation behavior at relatively high doping. It is attributed to reduction in impurity as well as recombination effects, as stated earlier. The saturation behavior observed in Fig. 5 illustrates a limit, *i.e.*, theoretical limit, associated with the Si-perovskite tandem cell. The results record a saturation of around 37.78% for the $BaTiO_3$/$CsPbCl_3$/$MAPbBr_3$/$CH_3NH_3PbI_3$/c-Si tandem structure. This value can be evaluated as good penetration of the theoretical limit for the Si-counter cell. In addition, it shows more double boosting against the reported Si-cell of 18% efficiency.

4. Conclusion

In conclusion, the results of work demonstrated in this paper provide an attempt to optimize the performance of a Si-perovskite tandem cell $BaTiO_3$/$CsPbCl_3$/$MAPbBr_3$/$CH_3NH_3PbI_3$/c-Si. Four inputs related to the c-Si cell are linked in an ultra-huge dataset to the overall PCE. The dataset is trained using the random forest machine learning model. Predictions conclude the occurrence of a clipping PCE close to 37.78%, which can represent a ceiling limit for the proposed tandem multi-junction cell.

Acknowledgment

The authors would like to acknowledge the support and contribution of the STDF in this work as a part of the STDF Project entitled “Mesostructured Based Solar Cells for Smart Building Applications”, Project ID#33502.

Conflict of interest

No conflict of interest exists in the submission of this manuscript, and all the authors approve the manuscript for publication. I want to declare on behalf of my co-authors that the work described was original research that has not been published previously and is not under consideration for publication elsewhere, in whole or in part. All the authors listed have approved the manuscript that is enclosed.

References

1. Zhang J., Lu L., Zhang J. *et al.* Monolithic perovskite/silicon tandem solar cells with optimized front zinc doped indium oxides and industrial textured silicon heterojunction solar cells. *J. Alloys Compd.* 2023. **932**. P. 167640. https://doi.org/10.1016/j.jallcom.2022.167640.
2. Zeder S., Ruhstaller B., Aeberhard U. Assessment of photon recycling in perovskite solar cells by fully coupled optoelectronic simulation. *Phys. Rev. Appl.* 2022. **17**, No 1. P. 014023. https://doi.org/10.1103/PhysRevApplied.17.014023.
3. Sharma R., Sharma A., Agarwal S., Dhaka M. Stability and efficiency issues, solutions and advancements in perovskite solar cells: a review. *Solar Energy*. 2022. **244**. P. 516–535. https://doi.org/10.1016/j.solener.2022.08.001.

4. Saikia D., Bera J., Betal A., Sahu S. Performance evaluation of an all inorganic $CsGeI_3$ based perovskite solar cell by numerical simulation. *Opt. Mater*. 2022. **123**. P. 111839. https://doi.org/10.1016/j.optmat.2021.111839.
5. Najafi M., Di Giacomo F., Zhang D. *et al.* Highly efficient and stable flexible perovskite solar cells with metal oxides nanoparticle charge extraction layers. *Small*. 2018. **14**, No 12. P. 1702775. https://doi.org/10.1002/smll.201702775.
6. Kim J.Y., Lee J.-W., Jung H.S., Shin H., Park N.-G. High-efficiency perovskite solar cells. *Chem. Rev.* 2020. **120**, No 15. P. 7867–7918. https://doi.org/10.1021/acs.chemrev.0c00107.
7. Yi C., Wu Y., Gao Y., Du Q. Tandem solar cells efficiency prediction and optimization via deep learning. *Phys. Chem. Chem. Phys.* 2021. **23**, No 4. P. 2991–2998. https://doi.org/10.1039/D0CP05882C.
8. Riedel M., Höfs S., Ruff A. *et al*. A tandem solar biofuel cell: harnessing energy from light and biofuels. *Angew. Chem.* 2021. **133**, No 4. P. 2106–2111. https://doi.org/10.1002/ange.202012089.
9. Nguyen D.C., Sato K., Hamada M. *et al*. Annual output energy harvested by building-integrated photovoltaics based on the optimized structure of 2-terminal perovskite/silicon tandem cells under realistic condition. *Solar Energy*. 2022. **241**. P. 452–459. https://doi.org/10.1016/j.solener.2022.06.018.
10. Messmer C., Tutsch L., Pingel S. *et al.* Optimized front TCO and metal grid electrode for module-integrated perovskite-silicon tandem solar cells. *Prog. Photovolt.: Res. Appl*. 2022. **30**, No 4. P. 374–383. https://doi.org/10.1002/pip.3491.
11. Kim C.U., Yu J.C., Jung E.D. *et al.* Optimization of device design for low cost and high efficiency planar monolithic perovskite/silicon tandem solar cells. *Nano Energy*. 2019. **60**. P. 213–221. https://doi.org/10.1016/j.nanoen.2019.03.056.
12. Chen B., Wang P., Li R. *et al.* Composite electron transport layer for efficient *n-i-p* type monolithic perovskite/silicon tandem solar cells with high open-circuit voltage. *J. Energy Chem.* 2021. **63**. P. 461–467. https://doi.org/10.1016/j.jechem.2021.07.018.
13. Palmstrom A.F., Eperon G.E., Leijtens T. *et al.* Enabling flexible all-perovskite tandem solar cells. *Joule*. 2019. **3**, No 9. P. 2193–2204. https://doi.org/10.1016/j.joule.2019.05.009.
14. Duong T., Wu Y., Shen H. *et al.* Rubidium multication perovskite with optimized bandgap for perovskite-silicon tandem with over 26% efficiency. *Adv. Energy Mater.* 2017. **7**, No 14. P. 1700228. https://doi.org/10.1002/aenm.201700228.
15. Li F., Peng X., Wang Z. *et al.* Machine learning (ML)-assisted design and fabrication for solar cells. *Energy & Environmental Materials.* 2019. **2**, No 4. P. 280–291. https://doi.org/10.1002/eem2.12049.
16. Mahran A.M., Abdellatif S.O. Investigating the performance of mesostructured based solar cells under indoor artificial lighting. 2*021 Int. Telecommun. Conf. (ITC-Egypt)*, Alexandria, Egypt, 2021. P. 1–5. https://doi.org/10.1109/ITC-Egypt52936.2021.9513924.
17. Mahran A.M., Abdellatif S.O. Optoelectronic modelling and analysis of transparency against efficiency in perovskites/dye-based solar cells. *2021 Int. Conf. on Microelectronics (ICM)*, New Cairo City, Egypt, 2021. P. 178–181. https://doi.org/10.1109/ICM52667.2021.9664924.
18. Ismail Z.S., Sawires E., Amer F.Z., Abdellatif S.O. Investigating the capacitive properties of all-inorganic lead halides perovskite solar cells using energy band diagrams. *2022 IEEE Int. Conf. on Semiconductor Electronics (ICSE)*, Kuala Lumpur, Malaysia, 2022. P. 45–48. https://doi.org/10.1109/ICSE56004.2022.9863109.
19. Eid A.A., Ismail Z.S., Abdellatif S.O. Optimizing SCAPS model for perovskite solar cell equivalent circuit with utilizing Matlab-based parasitic resistance estimator algorithm. *2020 2nd Novel Intelligent and Leading Emerging Sciences Conference (NILES)*, Giza, Egypt, 2020. P. 503–507. https://doi.org/10.1109/NILES50944.2020.9257929.
20. Abdelaziz S., Zekry A., Shaker A., Abouelatta M. Investigating the performance of formamidinium tin-based perovskite solar cell by SCAPS device simulation. *Opt. Mater*. 2020. **101**. P. 109738. https://doi.org/10.1016/j.optmat.2020.109738.
21. Al-Sabana O., Abdellatif S.O. Optoelectronic devices informatics: Optimizing DSSC performance using random-forest machine learning algorithm. *Optoelectron. Lett*. 2022. **18**, No 3. P. 148–151. https://doi.org/10.1007/s11801-022-1115-9.
22. Al-Saban O., Abdellatif S.O. Optoelectronic materials informatics: Utilizing random-forest machine learning in optimizing the harvesting capabilities of mesostructured-based solar cells. *2021 Int. Telecommun. Conf. (ITC-Egypt)*, Alexandria, Egypt, 2021. P. 1–4. https://doi.org/10.1109/ITC-Egypt52936.2021.9513898.
23. Abdellatif S.O., Amr L., Kirah K., Ghali H.A. Experimental studies for glass light transmission degradation in solar cells due to dust accumulation using effective optical scattering parameters and machine learning algorithm. *IEEE J. Photovolt.* 2023. **13**, No 1. P. 158–164. https://doi.org/10.1109/JPHOTOV.2022.3226711.
24. Abdellatif S., Fathi A., Abdullah K. *et al*. Investigating the variation in the optical properties of TiO_2 thin-film utilized in bifacial solar cells using machine learning algorithm. *J. Photonics Energy.* 2022. **12**, No 2. P. 022202. https://doi.org/10.1117/1.JPE.12.022202.
25. Chakure A. *Implementing Random Forest Regression in Python: An Introduction*. Ed.: builtin, 2022.
26. R.B.C.P. Ltd, *Understanding Bias-Variance Tradeoff*. Ed.: RSGB Business Consultant Pvt. Ltd.
27. Schmiga C., Nagel H., Schmidt J. 19% efficient *n*-type Czochralski silicon solar cells with screen-printed aluminium-alloyed rear emitter. *Prog. Photovolt.: Res. Appl*. 2006. **14**, No 6. P. 533–539. https://doi.org/10.1002/pip.725.

Authors and CV

Moustafa Ganoub, born in 1988, graduated from Electrical Engineering department, Faculty of Engineering in Ain Shams University, 2010. He is currently enrolled as a M.Sc. Student in the renewable energy Programme in the British University in Egypt.
E-mail: pg.moustafa91710016@bue.edu.eg

Omar Al-Saban, born in 1999, graduated from Electrical Engineering department, Faculty of Engineering in the British University in Egypt, 2021. He is currently working as research assistant in the FalbLab, at the faculty of Engineering, in the British University in Egypt.
E-mail: omar158071@bue.edu.eg

Sameh O. Abdellatif, born in 1987, (Senior Member, IEEE) received the B.Sc. degree in electronics and communication and the M.Sc. degree in semiconductor nanostructures from Ain Shams University, Cairo, Egypt, in 2009 and 2012, respectively. His Ph.D. work was funded by DAAD, it was focusing on the utilization of nano-photonic structures in enhancing solar cells efficiency. Currently, he is enrolled as Associate Professor with the Electrical Engineering Department, The British University in Egypt (BUE), where he is the Sub-Group Leader at the Fab Laboratory, Centre of Emerging Learning Technology (CELT). https://orcid.org/0000-0001-8677-9497

Khaled Kirah, born in 1962, Emeritus Professor at Engineering Physics and Mathematics, received the B.Sc. degree in electronics and communication and the M.Sc. degree in semiconductor nanostructures from Ain Shams University, Cairo, Egypt, in 1985 and 1994, respectively. His Ph.D. degree from the same university in 2000. https://orcid.org/0000-0001-5090-2529. E-mail: khaled.kirah@eng.asu.edu.eg

Hani A. Ghali, born in 1961, Prof. Ghali earned his B.Sc. in Electronics and Computer Engineering in 1983 from the Faculty of Engineering, Ain-Shams University, followed by M.Sc. in 1988 from the same University. He is the full professor in microwave systems and antennas. Prof. Ghali is the author and co-author of more than 150 publications. His main scientific interests include development of solar cells and studying their performances. E-mail: hani.amin@bue.edu.eg, https://orcid.org/0000-0001-8525-551X

Authors' contributions

Moustafa Ganoub: formal analysis, investigation, data curation (partially), writing – original draft, writing – review & editing, visualization.
Omar Al-Saban: software, writing – original draft.
Sameh O. Abdellatif: conceptualization, methodology, validation, formal analysis, investigation, resources, data curation, writing – original draft, writing – review & editing.
Khaled Kirah: review & editing, supervision.
Hani A. Ghali: review & editing, supervision.

Використання алгоритму машинного навчання для прогнозування межі ефективності перетворення потужності монолітної перовскітно-кремнієвої тандемної структури

M. Ganoub, O. Al-Saban, S.O. Abdellatif, K. Kirah, H.A. Ghali

Анотація. Тандемні структури були представлені на ринку фотовольтаїки для підвищення ефективності перетворення енергії (ЕПЕ). ЕПЕ елементів з одним гомо- або гетеропереходом, обмежується теоретичною межею, пов'язаною з шириною забороненої зони поглинаючого матеріалу. Масштабування одноперехідних елементів до багатоперехідних тандемних структур виходить за ці обмеження. Однією з перспективних тандемних структур є топологія перовскіт на кремнії. Si перехід використовується як тильний елемент, укритий зверху шарами перовскітів із урахуванням інженерних аспектів забороненої зони. Тут для дослідження ми вибрали тандемну структуру $BaTiO_3/CsPbCl_3/MAPbBr_3/CH_3NH_3PbI_3$/c-Si. У тандемних фотоелектричних елементах різні вхідні параметри можна налаштувати для максимізації ЕПЕ, що приводить до значного збільшення вхідних комбінацій. Такий великий набір даних безпосередньо відображає вимоги до обчислень, які необхідні для моделювання широкого діапазону комбінацій, і до тривалості цих обчислень. У цьому дослідженні ми використали нашу модель машинного навчання випадкового лісу з набором даних 3×10^6 точок з нашою оптоелектронною чисельною моделлю в SCAPS. За допомогою моделі машинного навчання можна оцінити максимальну межу ЕПЕ запропонованої тандемної структури на рівні приблизно 37,8%, що більш ніж удвічі перевищує зареєстровану ефективність кремнієвих елементів (18%).

Ключові слова: тандемні сонячні елементи, чисельне моделювання, перовскіти, алгоритм випадкового лісу, кристалічний кремній.